Narayan et al | Article 12066
J Pure Appl Microbiol. 2026. doi: 10.22207/JPAM.20.4.19
Received: 26 July 2026 | Accepted: 28 August 2026

P-ISSN: 0973-7510; E-ISSN: 2581-690X

RESEARCH ARTICLE OPEN ACCESS

Diosgenin as a Potential Therapeutic Agent for Bleomycin-Induced Pulmonary Fibrosis with Anti-Inflammatory, Antifibrotic and Antibacterial Activity

Ashwini Narayan[1], Souparnika H. Manjunath[1], Anil Kumar[2], B.S. Priya[3], Syed Baker[4], S. Niranjan Raj[4] and S. Nanjunda Swamy[1]*

[1]Department of Biotechnology, JSS Science and Technology University, Mysuru, Karnataka, India.
[2]Center for Research and Innovation, Department of Biotechnology, Adichunchanagiri School of Natural Science, Adichunchanagiri University, Nagamangala, Karnataka, India.
[3]DoS in Chemistry, University of Mysore, Manasagangotri, Mysuru, Karnataka, India.
[4]Department of Studies in Microbiology, Karnataka State Open University, Mysuru, Karnataka, India.

Abstract

Idiopathic pulmonary fibrosis (IPF) is a severe long disease characterized by excessive extracellular matrix deposition, chronic inflammation, and irreversible lung remodeling. The study conducted in vivo anti-inflammatory, antifibrotic and antibacterial activity against bleomycin induced pulmonary fibrosis in mice. Pulmonary fibrosis was induced by intratracheal bleomycin administration, followed by prophylactic and therapeutic treatment with diosgenin. Histopathological analysis revealed severe lung injury with a 3.3 fold increase in fibrotic burden, which was significantly attenuated by diosgenin. Pulmonary inflammation was reduced by 39% and 33% in the prophylactic and therapeutic groups, respectively, while collagen deposition decreased by 80%, comparable to nintedanib (84%). Diosgenin suppressed neutrophil extracellular trap formation, reducing citrullinated histone H3 (CitH3) by 30%-40%, and significantly downregulated fibronectin, α-smooth muscle actin (α-SMA), collagen type I (Col1), and monocyte chemoattractant protein-1 (MCP1). Although TGF-β mRNA expression increased, no corresponding reduction in TGF-β protein levels was observed, suggesting post-transcriptional regulation. Pharmacokinetic analysis demonstrated preferential lung accumulation at 10 mg/kg, whereas higher systemic exposure occurred at 30 mg per kg (mg/kg). Antibacterial activity was evaluated using broth dilution and agar well diffusion assays against *Escherichia coli*, *Bacillus subtilis*, *Bacillus cereus*, and *Salmonella typhi*. Diosgenin significantly inhibited bacterial growth and produced inhibition zones of 23, 22, 20, and 19 mm, respectively, demonstrating broad-spectrum antibacterial activity. Collectively, these findings identify diosgenin as a promising multi-target therapeutic candidate with anti-inflammatory, antifibrotic, and antibacterial properties for the treatment of pulmonary fibrosis and associated bacterial infections.

Keywords: Idiopathic Pulmonary Fibrosis, Bleomycin, Diosgenin, Anti-inflammation, Mouse Model, Antibacterial Activity

***Correspondence:** nanjundaswamy@jssstuniv.in

Citation: Narayan A, Manjunath SH, Kumar A, et al. Diosgenin as a Potential Therapeutic Agent for Bleomycin-Induced Pulmonary Fibrosis with Anti-Inflammatory, Antifibrotic and Antibacterial Activity. *J Pure Appl Microbiol.* Published online 11 November 2026. doi: 10.22207/JPAM.20.4.19

© The Author(s) 2026. **Open Access**. This article is distributed under the terms of the Creative Commons Attribution 4.0 International License which permits unrestricted use, sharing, distribution, and reproduction in any medium, provided you give appropriate credit to the original author(s) and the source, provide a link to the Creative Commons license, and indicate if changes were made.

INTRODUCTION

Idiopathic pulmonary fibrosis (IPF) represents a chronic and continuously progressive lung disease known by abnormal wound-healing processes. This is characterised by lung parenchyma damage, exhibiting diverse patterns of interstitial inflammation, cellular proliferation, and fibrosis within the alveolar wall and interstitium.[1] The aetiology of IPF remains unknown, further underscoring the complexity of this devastating and ultimately fatal pulmonary disorder.[2] It has been demonstrated that regardless of the signalling cascades that induce fibrosis, the outcome of these processes is the substantial increase of interstitial collagen, leading to scar formation and tissue fibrosis.[3] In the healing process of interstitial milieu, activated fibroblast/myofibroblast entities actively participate in the secretion of extracellular matrix (ECM) constituents, producing structural distortions in the lung architecture and an associated impairment of gas exchange.[4] These pathological processes ultimately culminate in progressive organ failure, with patients diagnosed with IPF facing a poor prognosis, reflected by an average survival duration of approximately 3-5 years.[5,6] Despite this regulatory milestone, the current therapeutic armamentarium available for the management of pulmonary fibrosis remains inadequate and is further compounded by the presence of adverse side effects.[7-9] As a terminal therapeutic option, lung transplantation offers the potential for prolonged survival; however, it is regarded as a last-resort intervention owing to its procedural complexity and substantial risk profile.[10] Moreover, fibrosis substantially influences various physiological processes, including tumour invasion and metastasis, chronic graft rejection, and the pathogenesis of numerous progressive myopathies.[11]

Despite the multiple hypotheses postulated by studies regarding potential etiological factors contributing to IPF, such as exposure to tobacco, environmental pollutants, viral infections, medication use, or a familial predisposition to IPF, the precise aetiology and underlying pathophysiological mechanisms of pulmonary fibrosis remain shrouded in mystery.[12,13] IPF predominantly afflicts the male population in comparison to females and typically affects individuals above the age of 50.[14] It is estimated that 20 out of every 100,000 males and 13 out of every 100,000 females suffer from IPF.[15] Extensive clinical investigations into anti-inflammatory and antifibrotic drugs for treating IPF have been conducted, employing diverse in-vivo models.[16,17] The American Thoracic Society has established formal guidelines for the preclinical assessment of antifibrotic therapeutic candidates.[18]

Intratracheal administration of Bleomycin, a cytostatic drug and chemotherapeutic antibiotic, is widely recognised as a gold standard and robust model for inducing pulmonary fibrosis in mice and has gained worldwide acceptance.[19] This model closely mimics the disease progression observed in humans.[20] It provides an ideal platform for the screening of candidate anti-inflammatory and antifibrotic agents, enabling rigorous comparative pharmacological evaluation between species.[21] However, it is important to note that repeated systemic administration of Bleomycin, as an adverse pharmacological effect, can elicit persistent pulmonary inflammation in certain patients, which may subsequently progress to fibrotic remodeling.[22,23]

Moreover, Bleomycin is reported to cause DNA damage in tumour cells.[24] The elevated levels of reactive oxygen species promote excessive synthesis of mature collagen fibrils, thereby initiating an inflammatory cascade that drives pulmonary toxicity, stimulates fibroblast activation, and ultimately leads to fibrotic remodeling.[25,26]

A recent study has highlighted Diosgenin's therapeutic potential in inhibiting transforming growth factor-beta (TGF-β1)/ Smad signalling and regulating epithelial-mesenchymal transition in experimental pulmonary fibrosis.[27] The present study extends these observations by evaluating the effects of diosgenin in bleomycin-induced pulmonary fibrosis using both prophylactic and therapeutic treatment regimens. In addition to assessing pulmonary fibrosis and collagen deposition, we investigated inflammatory responses, CitH3-associated neutrophil extracellular trap (NET) formation, fibrotic and inflammatory molecular markers, and the pulmonary and systemic exposure of diosgenin. The antibacterial activity of diosgenin was also evaluated to provide broader pharmacological characterization. Diosgenin, a

bioactive steroidal triterpene sapogenin found in various plant species, exhibits a range of medicinal properties, including hypolipidemic, hypoglycaemic, antioxidant, anti-inflammatory, and anti-proliferative activities.[28] Early research has also revealed its anti-proliferative properties in various cancer cell lines and its ability to induce apoptosis in cell lines associated with bone, breast, and liver cancers.[29-31] Diosgenin is primarily recognized for its capacity to modulate multiple cellular signaling pathways.[32] Diosgenin functions as a key precursor in the semi-synthetic production of steroidal drugs by pharmaceutical companies.[33] Based on these findings, Diosgenin may represent a promising therapeutic candidate for attenuating Bleomycin-induced fibrosis in C57BL/6 male mice.

MATERIALS AND METHODS

Experimental animal

The experiments were conducted with male mice (C57BL/6) weighing 20-24 g and 8-10 weeks old, obtained from Vivo BioTech (Taconic), Hyderabad, India. The mice were acclimatized to the animal facility for a period of one week before starting the experiments.

Ethical approval

All experimental protocols were reviewed and approved by the Institutional Animal Ethics Committee (IAEC) of Vaarunya Biolabs Pvt. Ltd. (VBPL/ IAEC/017/2022), in accordance with national guidelines for the care and use of laboratory animals. Efforts were made to minimize animal suffering and the number of animals used in each experiment.

Bleomycin mouse model development

Prior to experimentation, mice were quarantined for one week. Following quarantine, the mice were randomized, sensitized, and allocated into seven groups of 10 animals each.[34] The anesthesia protocol employed for intratracheal administration of Bleomycin induction entailed a combination of 3% O_2 and 2.5% Isoflurane, administered for 5 minutes.[35] The experimental protocol involved performing a neck dissection and administering a single dose of 50 µg of Bleomycin prepared in 50 µL of normal saline (1 mg/mL) via the intratracheal route.[36,37] On the other hand, the control group received only normal saline. The treatment group received an oral dose of Diosgenin from day 0-14 for the prophylactic study and day 8-14 for the therapeutic study. On day 14, animals were subjected to gross pathology.

Drug dosing experimental plan

A total of 70 mice were included in the study, with 10 mice allocated to each of seven experimental groups. Sixty mice in the disease-control and treatment groups received intratracheal administration of bleomycin on Day 0, followed by treatment with either diosgenin at doses of 10 or 30 mg/kg twice daily (b.i.d.) in the prophylactic and therapeutic groups or nintedanib at 60 mg/kg once daily (q.d.) as the positive control. The remaining 10 mice constituted the vehicle-control group and received saline only without bleomycin sensitization. On day 14, terminal sacrifice was conducted for the prophylactic and therapeutic groups (Supplementary Table S1). The experimental animals were monitored daily for clinical signs, and body weight was recorded twice weekly throughout the study.

Sample collection

Blood was collected by retro-orbital plexus for plasma, and all the surviving animals were sacrificed by CO_2 asphyxiation.[38] 70% ethanol was sprayed onto the chest region to make the surface clean. A midline incision was made in the chest region to facilitate the separation of lung tissue. The entire lung was carefully isolated from surrounding viscera and mesentery. Each lobe was then detached from the trachea. The right lower lobe of the lung was subsequently collected for histological analysis. The left diaphragmatic lung lobe was flash frozen in liquid nitrogen and stored at -80 °C until processed further for total collagen analysis, the right superior lung lobe for other inflammatory and molecular analysis[39] (Supplementary Figure S1).

Lung collagen determination

Total amount of lung collagen was quantified using the Sirius Red Detection Kit (Chondrex), in accordance with the manufacturer's protocol with minor procedural modifications. 100 mg of lung tissue underwent homogenization in 100 µl of milliQ (1 g/ml) solution containing 100

µl of pepsin (1 mg/mL in 0.05 M acetic acid). This homogenized mixture was incubated overnight at 4 °C overnight on rotary shaker, followed addition of 500 µl of Sirius Red Solution into the tissue lysates and collagen standards. Lysates were subsequently incubated at room temperature for 2 hours followed by centrifugation of 10,000 g for 25 minutes at 10 °C. 500 µl of a wash solution was added to the resulting pellet and centrifuged at 10,000 g for 15 minutes. The total collagen content was then extracted using 250 µl of extraction buffer. Of this extract, 200 µl was transferred to a 96-well plate, and the optical density was measured within the wavelength range of 510-550 nm.[40]

Citrullinated histone H3 analysis

The Citrullinated Histone H3 (CitH3) Elisa Kit provided by Cayman Chemicals was utilized according to the manufacturer's directions. The activity of CitH3 was assessed in 100 µl of tissue lysates, and the optical density was quantified at a wavelength of 450 nm. Citrullination activity ng/µl was normalized against protein concentration mg/ml and represented as ng/mg.[41] Background correction was done by nullifying values from blank well to all the samples and standards. Sample lysate concentration was derived from a standard curve.

Lung myeloperoxidase activity

Myeloperoxidase (MPO) activity was quantified in 100 mg of lung tissue using the Mouse Myeloperoxidase DuoSet ELISA kit (R&D Systems), following the manufacturer's instructions with minor methodological adjustments. The resulting MPO concentrations (pg/mL) were normalized to the corresponding total protein content (mg/mL) and expressed as pg of MPO per mg of protein.[42]

Lung TGF-β activity

TGF-β1 levels were quantified using a Mouse TGF-β1 DuoSet ELISA kit (R&D Systems) in 100 µL of tissue lysate, following the manufacturer's protocol. The measured concentration (in pg/mL) was normalized to the total protein content (mg/mL) of each sample and expressed as pg of TGF-β1 per mg of protein.[43]

RNA extraction and Real-Time PCR

100 mg of frozen lung tissue was taken for the extraction of RNA using the Sigma TRI Reagent®. Phase separation was carried out at room temperature in chloroform, followed by RNA precipitation in 70% ethanol. RNA concentration and quality were assessed using a NanoDrop. 4 µg of RNA were used to synthesise complementary DNA (cDNA) using the iScriptTM cDNA Synthesis Kit from Bio-Rad. RT-PCR was carried out by StepOnePlus Real-Time PCR apparatus from Applied Biosystems. Gene mRNA levels were measured using Applied Biosystems SYBR Green PCR Master Mix.[44] The mRNA levels of each sample were expressed fold above control animals that received no treatment at all and were normalised to TBP (TATA-binding protein).[45] PCR primers details have been given in the supplementary Table S2.

Histopathological evaluation of lungs

Gomori's Trichrome Staining was employed to visualize collagen fibers within lung tissue using the Richard Allan kit from Thermo Scientific.[46] For standard paraffin embedding, 5 micron serial sections were created using a microtome and these sections were subsequently stained with Gomori Trichrome Stain from Millipore following the manufacturer's guidelines.

All investigations and evaluations were conducted using light microscopy for qualitative analysis. The assessment of lung fibrosis was performed according to the Histological Lung Fibrosis Grading System based on the Modified Ashcroft scale. A total of 20 microscopic fields per slide were examined to determine the severity of lung fibrosis. Each field was assigned a score ranging from 0 (indicating normal lung) to 8 (indicating total fibrosis) using the modified Ashcroft scoring method.[47] Histopathological assessment and scoring were performed by a qualified pathologist who was blinded to the treatment allocation to minimize potential observer bias. Additionally, Hematoxylin and Eosin staining of lung sections was carried out, and the resulting slides were reviewed and subjectively analyzed for general signs of inflammation.[48] Briefly, the architecture of the lungs was assessed and scored for inflammation.

A score of 0-4 was assigned for inflammation scoring, where 0 indicates no inflammation, 1 indicates mild inflammation, 2 shows moderate inflammation, and 3 and 4 indicate severe and extreme inflammation.[49]

Pharmacokinetics (PK) evaluation

On day 14, two hours following the final administration of diosgenin at doses of 10 mg/kg and 30 mg/kg, animals were euthanized and subjected to necropsy. Blood samples were collected for pharmacokinetic evaluation, and lung tissues were excised. Half of the right lung lobe was allocated for drug exposure analysis. Tissue homogenates were prepared and analyzed for diosgenin concentrations using liquid chromatography coupled with tandem mass spectrometry (LC MS/MS).[50]

Statistical analysis

The data were presented as the mean ± standard error of the mean (SEM), and all statistical analysis was conducted using GraphPad Prism® 5 software. The research parameters were compared between the treatment groups and their corresponding vehicle control groups using One-way ANOVA, followed by either Dunnett's or Bonferroni post-test. A P-value ($P < 0.05$) was deemed to be statistically significant.

Antibacterial assay

The antibacterial activity of the 10 mg per ml Diosgenin dissolved in 50% methanol was evaluated using well diffusion and broth dilution assays. In the well diffusion method, sterile nutrient agar plates were swabbed with the test pathogens (*Escherichia coli*-NCTC 12923) (*Bacillus subtilis*-NCTC-10400) (*Bacillus cereus*-NCTC 7464) (*Salmonella typhi*-NCTC 8385), wells (10 mm diameter) were prepared using a sterile cork borer, and 10 mg per ml Diosgenin was added to each well. Plates were incubated at 37 °C for 24 hours, after which the zone of inhibition was measured and compared with amoxycillin (1 µg/mL) and methanol as controls. In the broth dilution assay, sterile nutrient broth containing 10 mg per

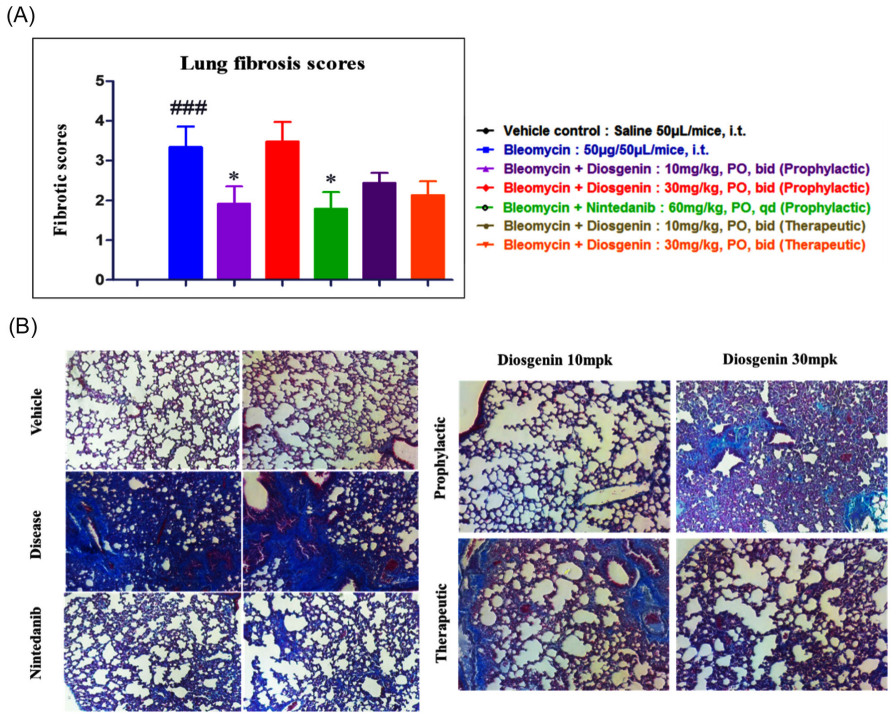


Figure 1. Lung fibrosis scoring in all tested groups compared to the Bleomycin control group. (A). Representative images for collagen fibers indicating fibrotic mass across all tested study groups (B). Trichrome Gomori staining sections were performed for fibrosis scoring

ml Diosgenin and 10 µL of the test pathogen was incubated at 37 °C for 24 hours, with appropriate positive and negative controls. Microbial growth was assessed by measuring turbidity at 600 nm.[51] All test pathogens were procured from herbal drug technological laboratory, Department of Studies in Microbiology, University of Mysore. The standard inoculum was prepared with McFarland dilution methods in accordance with Clinical and Laboratory Standards Institute (CLSI) guidelines. The antibacterial assay was performed in triplicate.

RESULTS

Bleomycin induced the disruption of lung architecture

Intratracheal administration of Bleomycin successfully induced pulmonary fibrosis in mice, as evidenced by Trichrome Gomori staining of lung sections. Quantitative analysis revealed a 3.3 fold increase in fibrotic deposition in Bleomycin treated animals compared to vehicle controls. Histopathological scoring using the Ashcroft scale demonstrated fibrotic indices exceeding three, consistent with severe fibrotic remodelling. Morphological examination further confirmed extensive structural damage, characterized by obstruction of alveolar spaces and pronounced thickening of fibrotic septal walls, resulting in marked disruption of normal lung architecture (Figure 1, Supplementary Figure S2).

Diosgenin diminishes bleomycin-induced lung inflammation

Intratracheal administration of Bleomycin resulted in a significant induction of pulmonary

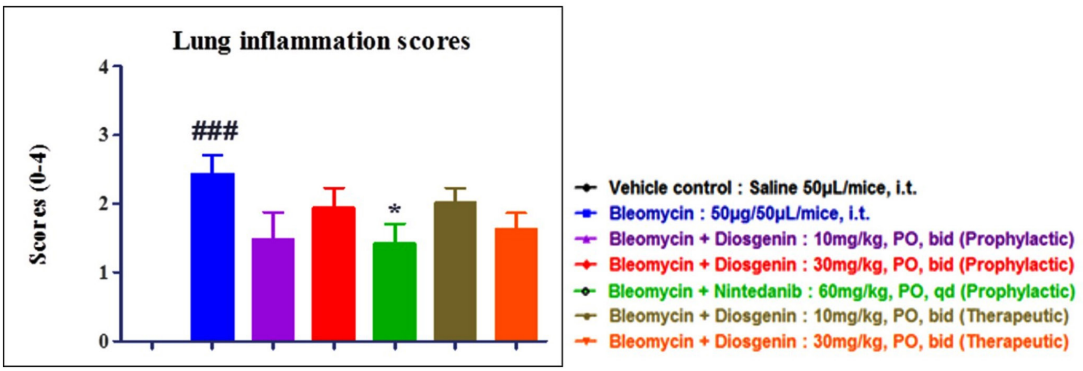


Figure 2. Diosgenin inhibited the inflammation induced by Bleomycin. Inflammation scoring in Bleomycin sensitized group. Data are shown as Mean ± SEM. ### P < 0.001 compared to Vehicle control and * P < 0.05 compared to Disease control. One Way ANOVA, Dunnett's multiple comparison tests

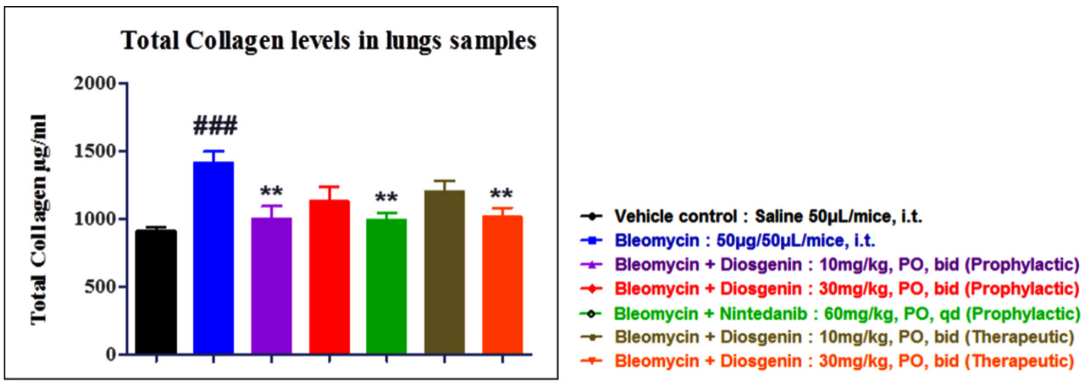


Figure 3. Tissue collagen levels tested in different groups (n = 10). Data are shown as Mean ± SEM; ** P < 0.01 vs. Disease control; ### P < 0.001 compared to Vehicle control. One Way ANOVA and Dunnett's tests for multiple comparisons.

inflammation, with treated mice exhibiting a 2.4 fold increase in inflammatory levels compared to vehicle controls. Administration of Diosgenin demonstrated notable anti-inflammatory activity. Specifically, prophylactic treatment at 10 mg/kg and therapeutic treatment at 30 mg/kg reduced inflammation by 39% and 33%, respectively. Additional dose dependent effects were observed, with Diosgenin at 30 mg/kg (prophylactic) and 10 mg/kg (therapeutic) lowering inflammation by

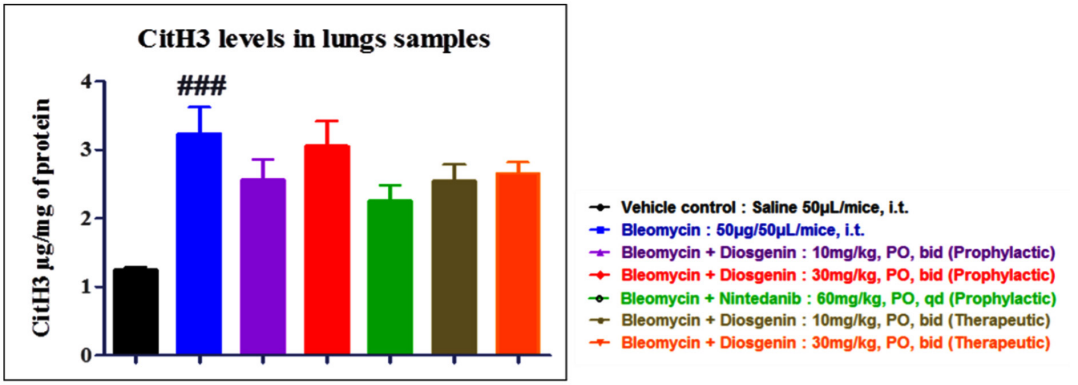


Figure 4. Citrulline levels in the lung lysates of tested groups (n = 10). Data represented as Mean ± SEM, ### P < 0.001 compared to Vehicle control. One Way ANOVA, Dunnett's multiple comparison tests

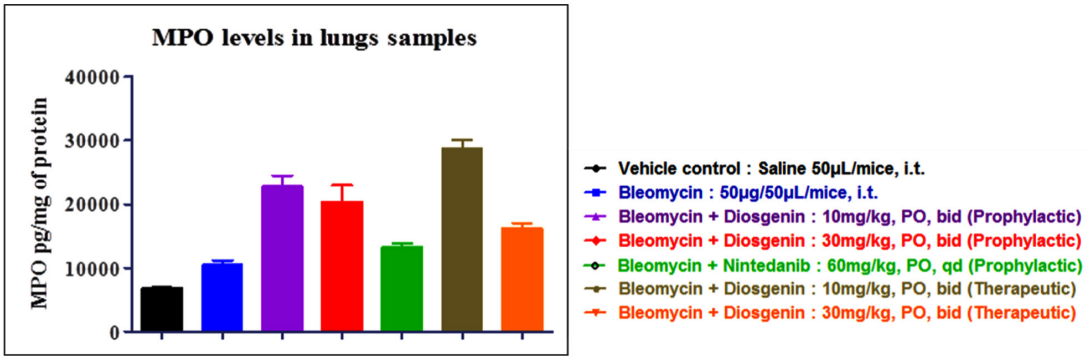


Figure 5. Myeloperoxidase activity in all treated groups. Data represented as Mean ± SEM. One Way ANOVA, Dunnett's multiple comparison tests

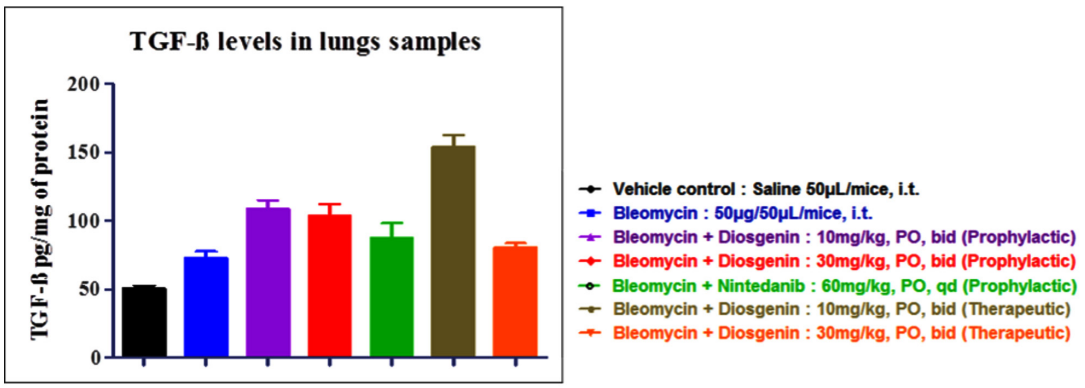


Figure 6. TGFβ expression levels in all tested groups. Data represented as Mean ± SEM. One Way ANOVA, Dunnett's multiple comparison tests

20% and 17%, respectively. The antifibrotic agent nintedanib, used as a positive control, reduced inflammation by 42%, confirming its efficacy in this model. Importantly, neither prophylactic nor therapeutic Diosgenin treatments produced significant changes in body weight, indicating good tolerability of the compound (Figure 2; Supplementary Figure S3).

Diosgenin attenuates collagen levels in Bleomycin-induced lung fibrosis

Excessive deposition of collagen within the pulmonary extracellular matrix was observed to impair lung function, leading to alveolar deformation and structural deterioration. Intratracheal administration of Bleomycin induced a 1.5 fold increase in collagen content compared to vehicle treated controls, confirming the establishment of fibrotic pathology. Treatment with Diosgenin markedly attenuated collagen accumulation, with prophylactic administration at 10 mg/kg and therapeutic administration at 30 mg/kg reducing collagen levels by approximately 80% relative to the Bleomycin group. As a reference control, the antifibrotic agent nintedanib demonstrated robust efficacy, lowering collagen deposition by 84%. These findings highlight the significant antifibrotic potential of Diosgenin, comparable to that of nintedanib, in mitigating Bleomycin induced pulmonary fibrosis (Figure 3).

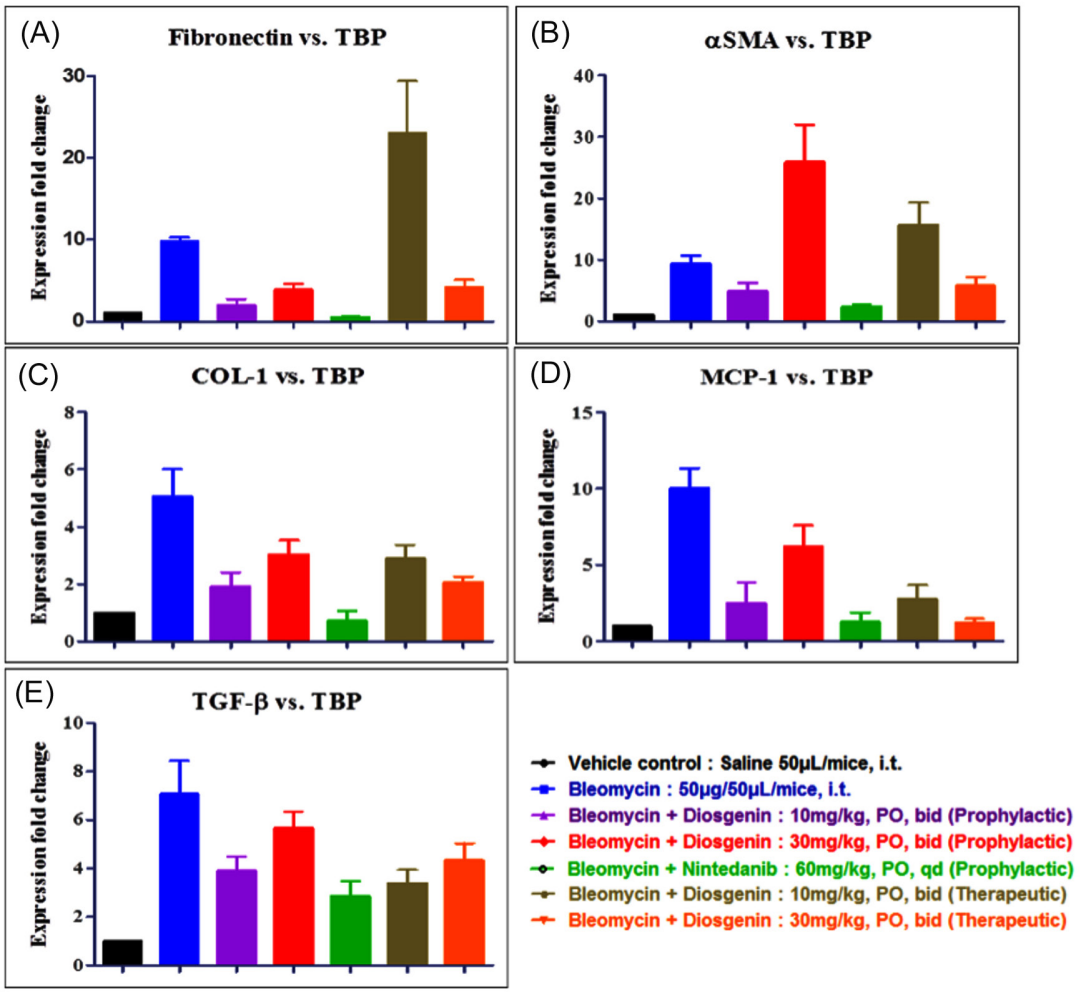


Figure 7. Expression analysis of biomarkers such as (A) Fibronectin, (B) αSMA, (C) Col1, (D) MCP1 and (E) TGF-β in mice induced with Bleomycin. Data represented as Mean ± SEM; One Way ANOVA, Dunnett's multiple comparison tests

Diosgenin alleviates NETosis in Bleomycin-induced lung fibrosis

Bleomycin administration markedly upregulated neutrophil extracellular trap (NET) formation in the lungs, contributing to enhanced inflammatory and fibrotic responses. Elevated levels of citrullinated histone H3 (CitH3), a key biomarker of NETosis, were observed in bleomycin treated mice, confirming the activation of NET mediated pathways in pulmonary fibrosis. Treatment with Diosgenin significantly attenuated NETosis, producing a 30%-40% reduction in CitH3 expression in both prophylactic and therapeutic groups. Notably, the magnitude of reduction achieved with Diosgenin was comparable to that observed with the antifibrotic agent nintedanib, which served as a positive control. These findings suggest that Diosgenin effectively mitigates NETosis driven fibrotic progression in this model (Figure 4).

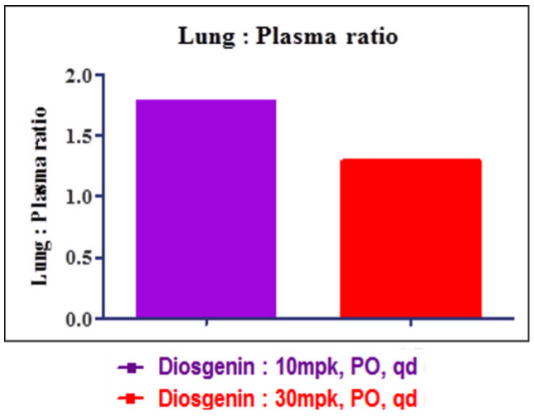


Figure 8. PK evaluation for lung plasma ratio in lung tissue lysates dosed with 10 mg/kg and 30 mg/kg Diosgenin. One Way ANOVA, Dunnett's multiple comparison tests

Diosgenin reduces the MPO levels in Bleomycin-induced lung fibrosis mice

Myeloperoxidase (MPO), a neutrophil derived enzyme, was quantified as a biochemical marker of pulmonary inflammation. Bleomycin administration resulted in a 1.5 fold elevation of MPO levels compared to vehicle treated controls, consistent with increased neutrophil infiltration and activity in the lung tissue. In contrast, Diosgenin treatment at both prophylactic (10 mg/kg) and therapeutic (30 mg/kg) doses did not produce significant changes in MPO levels, indicating that Diosgenin did not modulate neutrophil associated inflammatory responses under these experimental conditions (Figure 5).

Diosgenin on tissue TGF-β levels in lung fibrosis mice

Bleomycin administration resulted in a 1.4 fold elevation of transforming growth factor β (TGFβ) protein levels compared to vehicle controls, consistent with activation of fibrotic signaling pathways. Neither diosgenin nor nintedanib treatment produced a measurable reduction in TGFβ protein levels across the tested groups. Interestingly, diosgenin treatment was associated with increased TGFβ mRNA expression in the therapeutic cohorts, with a 2.1 fold rise at 10 mg/kg and a 1.1 fold rise at 30 mg/kg relative to controls. Similarly, nintedanib treatment led to a

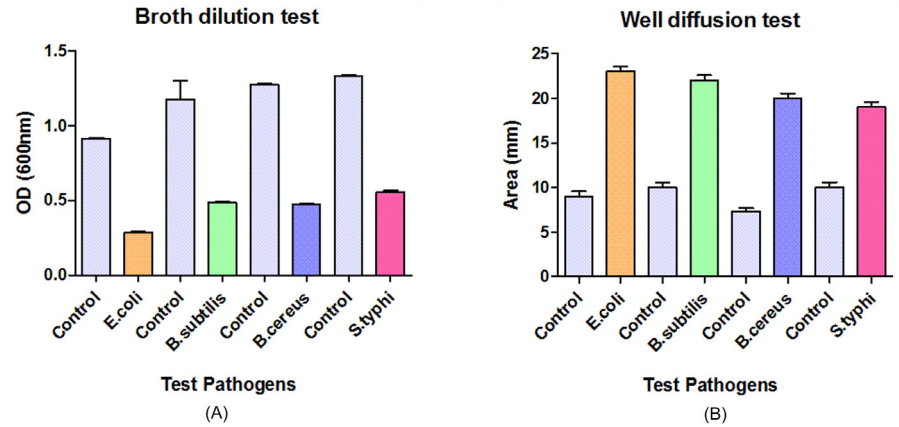


Figure 9. Antibacterial activity of diosgenin against the test pathogens. (A) Broth dilution (B) Well diffusion

1.2 fold increase in TGFβ mRNA expression. These findings suggest that while both agents attenuate fibrosis through other mechanisms, they may exert complex regulatory effects on TGFβ transcriptional activity without reducing protein abundance (Figure 6).

Effect of Diosgenin on lung fibrosis biomarkers

Bleomycin administration significantly elevated the mRNA expression of key fibrotic biomarkers, including fibronectin, α smooth muscle actin (αSMA), collagen type I (Col1), and monocyte chemoattractant protein 1 (MCP1), consistent with progressive fibrotic remodeling in the lung. Treatment with diosgenin markedly attenuated the expression of these markers, demonstrating its antifibrotic potential. The magnitude of reduction achieved with diosgenin was comparable to that observed with nintedanib, the reference antifibrotic agent. Importantly, diosgenin treatment provided sustained protection against fibrosis, preserving lung architecture and mitigating fibrotic progression up to 14 days following Bleomycin challenge (Figure 7).

Analysis of diosgenin lung and plasma exposure

Analysis of Diosgenin Lung and Plasma Exposure revealed that diosgenin concentrations were consistently higher in plasma than in lung tissue. At the 2 hrs post-dose sampling point, the 10 mg/kg group showed a higher lung-to-plasma concentration ratio than the 30 mg/kg group. These findings indicate dose-dependent differences in lung and plasma exposure at the sampled time point; however, concentration time profile studies are required to characterize the pharmacokinetic behavior of diosgenin and to determine whether tissue saturation occurs (Figure 8).

Antibacterial assay

The antibacterial activity of diosgenin was assessed using broth dilution and agar well diffusion assays against (*Escherichia coli*-NCTC 12923) (*Bacillus subtilis*-NCTC-10400) (*Bacillus cereus*-NCTC 7464) and (*Salmonella typhi*-NCTC 8385). In the broth dilution assay, treatment with diosgenin resulted in a marked reduction in bacterial growth compared with the untreated controls (amoxycillin and 50% methanol). The mean optical density (OD) values decreased from 0.914 ± 0.010 to 0.286 ± 0.007 for *Escherichia coli*, from 1.176 ± 0.221 to 0.487 ± 0.011 for *Bacillus subtilis*, from 1.276 ± 0.011 to 0.472 ± 0.010 for *Bacillus cereus*, and from 1.330 ± 0.009 to 0.558 ± 0.013 for *Salmonella typhi*, indicating substantial inhibition of bacterial growth. Consistent with these findings, the agar well diffusion assay demonstrated significantly larger zones of inhibition for diosgenin-treated samples than the controls. The mean inhibition zones increased from 9.0 ± 1.0-23.0 ± 1.0 mm against *Escherichia coli*, from 10.0 ± 1.0-22.0 ± 1.0 mm against *Bacillus subtilis*, from 7.3 ± 0.6-20.0 ± 1.0 mm against *Bacillus cereus*, and from 10.0 ± 1.0-19.0 ± 1.0 mm against *Salmonella typhi*. Among the test pathogens, the highest antibacterial activity was observed against *Escherichia coli* and *Bacillus subtilis*, with inhibition zones of up to 24 mm and 23 mm, respectively, demonstrating moderate activity against the test pathogens (Figure 9A and B).

DISCUSSION

Bleomycin, a chemotherapeutic antibiotic, induces pulmonary toxicity largely via oxidative injury and reduced inactivation by bleomycin hydrolase, which together promote epithelial cell damage in the lung.[52,53] Adamson's early work established systemic (repeated intraperitoneal) bleomycin administration as a method to generate interstitial fibrosis in rodents, a protocol that laid the foundation for later methodological refinements.[54] To better recapitulate the localized alveolar injury and parenchymal fibrosis seen in idiopathic pulmonary fibrosis (IPF), many subsequent studies adopted direct intratracheal instillation of bleomycin, which produces more rapid and reproducible lung injury.

The pathological evolution in intratracheal bleomycin models typically includes early alveolar epithelial cell death within the first 1-3 days, an inflammatory influx that peaks during the first week (roughly days 3-9), and matrix deposition and fibrotic remodeling that are readily apparent by ~day 14.[55] Because the bleomycin model yields consistent, dose-dependent injury with histologic

hallmarks (epithelial injury, inflammatory cell influx, collagen deposition) that resemble aspects of human IPF, it remains widely used in preclinical testing of antifibrotic candidates and mechanistic studies.[56] Nevertheless, important limitations persist: the model more closely resembles an acute or resolving fibrotic response rather than the progressive, irreversible fibrosis of human IPF, and outcomes are influenced by strain, age, route, and dosing of bleomycin factors that must be considered when translating preclinical findings.[57,58]

In this study, we observed pronounced pulmonary inflammation and subsequent fibrotic remodeling following bleomycin administration in mice. Consistent with canonical bleomycin-induced lung injury models, histological assessment revealed alveolar septal thickening, inflammatory cell infiltration, fibroblast proliferation, and marked collagen deposition in interstitial regions. These histopathological changes recapitulate key features of IPF in animal models.[20] Administration of Diosgenin and Nintedanib mitigated these bleomycin-induced alterations to differing extents: treatment with Diosgenin in a prophylactic regimen of 10 mg/kg led to an approximate 39% reduction in inflammatory pathology, while therapeutic administration at 30 mg/kg achieved around a 33% reduction in inflammation. In comparison, Nintedanib yielded a modestly greater attenuation (~42%) of lung injury under similar conditions. These findings align with recent reports demonstrating Nintedanib's capacity to ameliorate bleomycin-induced pulmonary fibrosis, reduce inflammatory cytokine expression, inhibit collagen accumulation, and restore antioxidant balance via modulation of the PI3K/Akt/mTOR pathway.[59] Moreover, studies have highlighted the importance of timing and dosing in antifibrotic interventions, as distinct regimens yield variable efficacy in reducing inflammation and fibrosis.[54] However, higher doses of Diosgenin in the prophylactic regimen (30 mg/kg), as well as lower doses in the therapeutic regimen (10 mg/kg), were less effective yielding only ~20% and ~17% reduction in lung inflammation, respectively. This dose- and time-dependent variability underscores the critical role of optimizing both the dosing strategy and treatment window to maximize therapeutic benefit in bleomycin-induced lung injury models. Collectively, our data reinforce the utility of the bleomycin mouse model for preclinical evaluation of candidate antifibrotic agents, while also emphasizing that the magnitude of therapeutic benefit is contingent on appropriate dose selection and timing of administration.

In our study, Bleomycin triggered a 3.3-fold increase in collagen deposition, reflecting robust fibrogenesis comparable to contemporary findings demonstrating reliable fibrosis induction with this model.[60] Both Diosgenin and Nintedanib reduced BLM-induced lung inflammation and fibrosis, though with different magnitudes, indicating that Diosgenin exhibits comparable therapeutic potential to Nintedanib. Inflammatory scoring showed 39% reduction in the prophylactic Diosgenin 10 mg/kg group and 33% reduction in the therapeutic 30 mg/kg group, while Nintedanib reduced inflammation by 42%. These reductions align with recent mechanistic work showing that antifibrotic interventions modulate innate immune activation and inflammatory cell recruitment in Bleomycin models.[61] Similarly, collagen quantification demonstrated that the prophylactic Diosgenin 10 mg/kg group and therapeutic Diosgenin 30 mg/kg group reduced fibrosis by 83% and 80%, respectively nearly equivalent to Nintedanib (84%). These outcomes reinforce that Diosgenin engages conserved antifibrotic pathways that reduce ECM accumulation, consistent with advanced fibrosis-targeting approaches reported recently.[62] Interestingly, prophylactic 30 mg/kg or therapeutic 10 mg/kg resulted in markedly lower protection (20% and 17% reductions, respectively), confirming that Diosgenin's therapeutic efficacy is highly dependent on intervention phase. This observation aligns with the current understanding that prophylaxis should target the inflammatory window before irreversible extracellular matrix remodeling ensues.[63] Therefore, strategic optimization of dosing and initiation timing is critical for maximizing clinical translation in fibrotic lung disease.

Neutrophil extracellular traps (NETs) are known mediators of pulmonary inflammation and fibrotic progression, quantified by evaluating citrullinated histone H3 (CitH3) expression. Bleomycin administration induced a marked elevation in CitH3 by ~2.6-fold, confirming enhanced NETosis activity. Treatment with

Nintedanib resulted in a substantial attenuation of this response, yielding an approximate 50% reduction in CitH3 levels. Diosgenin also significantly suppressed NET formation, demonstrating a moderate decline of ~30%-40%, thereby indicating its capacity to modulate NET-driven inflammatory mechanisms, albeit to a lesser extent than Nintedanib.[64]

Myeloperoxidase (MPO) activity is widely recognized as a robust biomarker for neutrophil-mediated inflammation in pulmonary fibrosis models. Elevated MPO levels following bleomycin exposure indicate neutrophil infiltration and activation during the acute inflammatory phase of lung injury, consistent with previous reports demonstrating enhanced MPO activity in BLM-induced experimental fibrosis.[65] In the present study, MPO levels increased approximately 1.5-fold in BLM-treated mice, confirming neutrophilic inflammation. However, Diosgenin administration did not significantly modify MPO levels in either prophylactic or therapeutic regimens, suggesting that its anti-inflammatory mechanism may not primarily target MPO-dependent pathways and instead may modulate alternative inflammatory or fibrotic signaling axes, as supported by prior investigations of Diosgenin in inflammatory disease models.[66]

Transforming growth factor β (TGFβ), a central mediator of fibrogenesis, was elevated by approximately 1.4 fold in bleomycin (BLM) treated mice, consistent with enhanced fibrotic signalling.[67] In contrast, diosgenin and nintedanib administration did not produce a corresponding reduction in TGFβ protein abundance across treatment groups.[68] Notably, a significant reduction in TGFβ mRNA expression was observed following diosgenin treatment, with prophylactic dosing at 10 mg/kg and 30 mg/kg resulting in ~52% and ~23% decreases, respectively. Therapeutic administration of diosgenin further reduced TGFβ mRNA levels by ~60% and ~45% at 10 mg/kg and 30 mg/kg, respectively. Thus, the reduction in TGFβ transcript abundance following diosgenin treatment was not accompanied by a corresponding reduction in tissue TGFβ protein levels at the time point examined. This difference may reflect the distinct temporal and regulatory relationships between transcript and protein abundance under the experimental conditions of the present study. These findings are consistent with prior reports demonstrating that TGFβ protein levels often remain stable despite antifibrotic interventions, while transcriptional regulation may be more sensitive to therapeutic modulation.[69]

Key fibrotic markers, including α-SMA, Col1, fibronectin, and MCP1, were significantly elevated in bleomycin-treated mice.[70] Diosgenin treatment markedly downregulated markers related to fibrogenesis and inflammation, indicating its potential to suppress myofibroblast activation and extracellular matrix (ECM) accumulation. In particular, the decrease in MCP-1 (a pro-inflammatory chemokine) was more pronounced in the therapeutic-regimen group, suggesting that Diosgenin is effective in attenuating fibrosis-associated inflammation even when administered after Bleomycin exposure.[71] Pharmacokinetic studies demonstrated that Diosgenin preferentially accumulates in lung tissue at a 10 mg/kg dose, whereas a 30 mg/kg dose results in higher systemic plasma levels, potentially reflecting lung tissue saturation at lower doses.[72] This targeted pulmonary distribution may contribute to localized antifibrotic activity while preserving systemic bioavailability.[73] Collectively, our results indicate that Diosgenin attenuates bleomycin-induced pulmonary fibrosis in a dose-dependent manner, reducing both inflammatory responses and extracellular matrix deposition.[74] Its efficacy in decreasing collagen accumulation is comparable to that of Nintedanib, highlighting its potential as a therapeutic antifibrotic agent.[75] Further investigations are warranted to delineate the molecular mechanisms underlying its antifibrotic effects and to optimize dosing regimens for future clinical translation. Natural products and plant-derived bioactive compounds may exhibit multidirectional pharmacological activities, including anti-inflammatory and antimicrobial effects, although the magnitude and mechanisms of these effects are highly compound- and context-dependent. In this context, the observed antibacterial activity of diosgenin further supports its potential as a bioactive compound with complementary antifibrotic and antimicrobial properties.[76-78] Collectively, these findings support further investigation of diosgenin as a potential therapeutic candidate for pulmonary fibrosis

and associated inflammatory and infectious complications.

CONCLUSION

In summary, the present study demonstrates that Diosgenin exerts pronounced anti-inflammatory and antifibrotic effects in a bleomycin-induced pulmonary fibrosis model. Both prophylactic and therapeutic administration of Diosgenin effectively attenuated fibrotic deposition within lung tissue, indicating its potential to not only impede disease progression but also facilitate tissue recovery. By reducing inflammation and extracellular matrix accumulation, the study also demonstrated antibacterial activity against test pathogens. Diosgenin may contribute to the preservation of pulmonary function and improved pathological outcomes. Future studies, including well-designed pre-clinical trials, are necessary to confirm the efficacy and safety of Diosgenin, thereby supporting its development as a potential therapeutic agent for pulmonary fibrosis.

SUPPLEMENTARY INFORMATION

Supplementary information accompanies this article at https://doi.org/10.22207/JPAM.20.4.19

Additional files: Tables S1, S2 and Figures S1-S3.

ACKNOWLEDGMENTS

The authors thank JSS Science and Technology University and Karnataka State Open University, Mysore, for providing the infrastructure to conduct this study.

CONFLICT OF INTEREST

The authors declare that there is no conflict of interest.

AUTHORS' CONTRIBUTION

AN conceptualized the study, applied methodology, and performed investigation. BSP and AN performed data analysis and data curation. SNS supervised the study and performed project administration. SNS and AN wrote the manuscript. SNS, SHM, SB, SNR and AK reviewed and edited the manuscript. All authors read and approved the final manuscript for publication.

FUNDING

None.

DATA AVAILABILITY

The datasets generated and/or analysed during the current study are available from the corresponding author on reasonable request.

ETHICS STATEMENT

This study was approved by the Institutional Animal Ethics Committee (IAEC), Vaarunya Biolabs Pvt. Ltd. (Approval No.: VBPL/IAEC/017/2022).

REFERENCES

1. Sgalla G, Iovene B, Calvello M, Ori M, Varone F, Richeldi L. Idiopathic pulmonary fibrosis: pathogenesis and management. *Respir Res.* 2018;19(1):32. doi: 10.1186/s12931-018-0730-2
2. Sankari A, Chapman K, Ullah S. *Idiopathic pulmonary fibrosis.* In: StatPearls [Internet]. StatPearls Publishing. 2024.
3. Moretti L, Stalfort J, Barker TH, Abebayehu D. The interplay of fibroblasts, the extracellular matrix, and inflammation in scar formation. *J Biol Chem.* 2022;298(2):101530. doi: 10.1016/j.jbc.2021.101530
4. Kamiya M, Carter H, Espindola MS, et al. Immune mechanisms in fibrotic interstitial lung disease. *Cell.* 2024;187(14):3506-3530. doi: 10.1016/j.cell.2024.05.015
5. Luppi F, Kalluri M, Faverio P, Kreuter M, Ferrara G. Idiopathic pulmonary fibrosis beyond the lung: understanding disease mechanisms to improve diagnosis and management. *Respir Res.* 2021;22(1):109. doi: 10.1186/s12931-021-01711-1
6. Wang T, Cui Z, Ou Y, et al. Post-marketing safety concerns with pirfenidone and nintedanib: an analysis of individual case safety reports from the FDA adverse event reporting system database and the Japanese adverse drug event report databases. *Front Pharmacol.* 2025;16:1530697. doi: 10.3389/fphar.2025.1530697
7. Salisbury ML, Conoscenti CS, Culver DA, et al. Antifibrotic drug use in patients with idiopathic pulmonary fibrosis: data from the IPF-PRO Registry. *Ann Am Thorac Soc.* 2020;17(11):1413-1423. doi: 10.1513/AnnalsATS.201912-880OC
8. Holtze CH, Freiheit EA, Limb SL, et al. Patient and site characteristics associated with pirfenidone and nintedanib use in the United States: an analysis of idiopathic pulmonary fibrosis patients enrolled in the Pulmonary Fibrosis Foundation Patient Registry. *Respir Res.* 2020;21:48. doi: 10.1186/s12931-020-1315-4
9. Dempsey TM, Payne S, Sangaralingham L, Yao X, Shah ND, Limper AH. Adoption of the antifibrotic medications pirfenidone and nintedanib for patients with idiopathic pulmonary fibrosis. *Ann Am Thorac Soc.* 2021;18(7):1121-1128. Cdoi: 10.1513/

AnnalsATS.202007-901OC
10. Zhao JY, Gouchoe DA, Schwartzman WE, et al. Long survival following lung transplantation: what matters? *Transplantology*. 2023;4(4):197-208. doi: 10.3390/transplantology4040019
11. Chen H, Xu X, Li J, et al. Decoding tumor-fibrosis interplay: mechanisms, impact on progression, and innovative therapeutic strategies. *Front Pharmacol.* 2024;15:1491400. doi: 10.3389/fphar.2024.1491400
12. Sauleda J, Nunez B, Sala E, Soriano JB. Idiopathic pulmonary fibrosis: epidemiology, natural history, phenotypes. *Med Sci*. 2018;6(4):110. doi: 10.3390/medsci6040110
13. Maher TM, Bendstrup E, Dron L, et al. Global incidence and prevalence of idiopathic pulmonary fibrosis. *Respir Res.* 2021;22(1):197. doi: 10.1186/s12931-021-01791-z
14. Sese L, Nunes H, Cottin V, et al. Gender differences in idiopathic pulmonary fibrosis: are men and women equal? *Front Med*. 2021;8:713698. doi: 10.3389/fmed.2021.713698
15. Sharif R. Overview of idiopathic pulmonary fibrosis (IPF) and evidence-based guidelines. *Am J Manag Care.* 2017;23(11 Suppl):S176-S182.
16. Liu H, Shen J, He C. Advances in idiopathic pulmonary fibrosis diagnosis and treatment. *Chin Med J Pulm Crit Care Med.* 2025;3(1):12-21. doi: 10.1016/j.pccm.2025.02.001
17. Vancheri C, Sciacca E, Muscato G, et al. Pharmacological treatment in idiopathic pulmonary fibrosis: current issues and future perspectives. *Multidiscip Respir Med.* 2024;19(1):982. doi: 10.5826/mrm.2024.982
18. Jenkins RG, Moore BB, Chambers RC, et al. An official American Thoracic Society workshop report: use of animal models for the preclinical assessment of potential therapies for pulmonary fibrosis. *Am J Respir Cell Mol Biol.* 2017;56(5):667-679. doi: 10.1165/rcmb.2017-0096ST
19. Tukhovskaya EA, Palikova YA, Severyukhina MS, et al. Comparison of the results of modeling pulmonary fibrosis in Sprague Dawley rats by intratracheal administration of bleomycin in the form of sulfate and chloride at a dose of 3 mg/kg. *Pharmaceuticals*. 2024;17(10):1360. doi: 10.3390/ph17101360
20. Ruscitti F, Ravanetti F, Essers J, et al. Longitudinal assessment of bleomycin-induced lung fibrosis by micro-CT correlates with histological evaluation in mice. *Multidiscip Respir Med.* 2017;12:8. doi: 10.1186/s40248-017-0089-0
21. Chaudhary NI, Schnapp A, Park JE. Pharmacologic differentiation of inflammation and fibrosis in the rat bleomycin model. *Am J Respir Crit Care Med.* 2006;173(7):769-776. doi: 10.1164/rccm.200505-717OC
22. Degryse AL, Tanjore H, Xu XC, et al. Repetitive intratracheal bleomycin models several features of idiopathic pulmonary fibrosis. *Am J Physiol Lung Cell Mol Physiol.* 2010;299(4):L442-L452. doi: 10.1152/ajplung.00026.2010
23. Saccone N, Bass J, Ramirez ML. Bleomycin-induced lung injury after intravenous iron administration. *Cureus.* 2022;14(7):e26864. doi: 10.7759/cureus.27531
24. Czaja M, Skirlinska-Nosek K, Adamczyk O, et al. Raman research on bleomycin-induced DNA strand breaks and repair processes in living cells. *Int J Mol Sci.* 2022;23(7):3524. doi: 10.3390/ijms23073524
25. Allawzi A, Elajaili H, Redente EF, Nozik-Grayck E. Oxidative toxicology of bleomycin: role of the extracellular redox environment. *Curr Opin Toxicol.* 2019;13:68-73. doi: 10.1016/j.cotox.2018.08.001
26. Liborio-Ramos S, Barbosa-Matos C, Fernandes R, Borges-Pereira C, Costa S. Interstitial macrophages lead early stages of bleomycin-induced lung fibrosis and induce fibroblast activation. *Cells.* 2023;12(3):402. doi: 10.3390/cells12030402
27. Dinesh Babu V, Suresh Kumar A, Sudhandiran G. Diosgenin inhibits TGF-β1/Smad signaling and regulates epithelial mesenchymal transition in experimental pulmonary fibrosis. *Drug Chem Toxicol.* 2022;45(3):1264-1275. doi: 10.1080/01480545.2020.1814803
28. Jesus M, Martins AP, Gallardo E, Silvestre S. Diosgenin: recent highlights on pharmacology and analytical methodology. *J Anal Methods Chem.* 2016;2016:4156293. doi: 10.1155/2016/4156293
29. Long C, Chen J, Zhou H, et al. Diosgenin exerts its tumor suppressive function via inhibition of Cdc20 in osteosarcoma cells. *Cell Cycle.* 2019;18(3):346-358. doi: 10.1080/15384101.2019.1568748
30. Ren QL, Wang Q, Zhang XQ, et al. Anticancer activity of diosgenin and its molecular mechanism. *Chin J Integr Med.* 2023;29(8):738-749. doi: 10.1007/s11655-023-3693-1
31. Yu H, Liu Y, Niu C, Cheng Y. Diosgenin increased DDX3 expression in hepatocellular carcinoma. *Am J Transl Res.* 2018;10(11):3590-3599.
32. Semwal P, Painuli S, Abu-Izneid T, et al. Diosgenin: an updated pharmacological review and therapeutic perspectives. *Oxid Med Cell Longev.* 2022;2022:1035441. doi: 10.1155/2022/1035441
33. Hussain MS, Fareed S, Ansari S, Rahman MA, Ahmad IZ, Saeed M. Current approaches toward production of secondary plant metabolites. *J Pharm Bioallied Sci.* 2012;4(1):10-20. doi: 10.4103/0975-7406.92725
34. Gul A, Yang F, Xie C, et al. Pulmonary fibrosis model of mice induced by different administration methods of bleomycin. *BMC Pulm Med.* 2023;23(1):91. doi: 10.1186/s12890-023-02349-z
35. Shaghaghi H, Kadlecek S, Deshpande C, et al. Metabolic spectroscopy of inflammation in a bleomycin-induced lung injury model using hyperpolarized 1-^{13}C pyruvate. *NMR Biomed.* 2014;27(8):939-947. doi: 10.1002/nbm.3139
36. Murgo A, Bignami F, Federico G, et al. Harnessing the translational power of bleomycin model: new insights to guide drug discovery for idiopathic pulmonary fibrosis. *Front Pharmacol.* 2023;14:1303646. doi: 10.3389/fphar.2023.1303646
37. Kadam AH, Schnitzer JE. Highly calibrated relationship between bleomycin concentrations and facets of the active phase fibrosis in classical mouse bleomycin model. *Int J Mol Sci.* 2024;25(22):12300. doi: 10.3390/ijms252212300

38. Herling AW, Maas J, Seeger K. Guidelines for the care and use of laboratory animals. In: Vogel HG, Vogel WH, eds. *Drug Discovery and Evaluation: Pharmacological Assays.* Springer; 1997:726-740. doi: 10.1007/978-3-662-03333-3_14
39. Morton J, Snider TA. Guidelines for collection and processing of lungs from aged mice for histological studies. *Pathobiol Aging Age Relat Dis.* 2017;7(1):1313676. doi: 10.1080/20010001.2017.1313676
40. Szasz C, Pap D, Szebeni B, et al. Optimization of Sirius Red-based microplate assay to investigate collagen production in vitro. *Int J Mol Sci.* 2023;24(24):17435. doi: 10.3390/ijms242417435
41. Dong T, Ouyang W, Yu X, et al. Synergistic inhibition of CitH3 and S100A8/A9: a novel therapeutic strategy for mitigating sepsis-induced inflammation and lung injury. *Int J Immunopathol Pharmacol.* 2025;39:03946320251338661. doi: 10.1177/03946320251338661
42. Adamson IY. Pulmonary toxicity of bleomycin. *Environ Health Perspect.* 1976;16(1):119-125. doi: 10.1289/ehp.7616119
43. Ghafoory S, Varshney R, Robison T, et al. Platelet TGF-β1 deficiency decreases liver fibrosis in a mouse model of liver injury. *Blood Adv.* 2018;2(5):470-480. doi: 10.1182/bloodadvances.2017010868
44. Niehof M, Hildebrandt T, Danov O, et al. RNA isolation from precision-cut lung slices (PCLS) from different species. *BMC Res Notes.* 2017;10(1):121. doi: 10.1186/s13104-017-2447-6
45. Mishal R, Meléndez-Zajgla J, Rueda-Zarazúa B, et al. RNA-seq analysis of wild-type and mutated TBPL1 gene in breast cancer cell lines through CRISPR/Cas9 approach reveals novel molecular signatures. *Sci Rep.* 2025;15(1):37578. doi: 10.1038/s41598-025-11634-2
46. Ryota M. Techniques of trichrome stains in histopathology and decoding fibrosis in liver, heart, and lungs. *J Interdiscip Histopathol*. 2023;11(11):1-2
47. Hubner RH, Gitter W, Eddine El Mokhtari N, et al. Standardized quantification of pulmonary fibrosis in histological samples. *Biotechniques*. 2008;44(4):507-517. doi: 10.2144/000112729
48. Zhou X, Moore BB. Lung section staining and microscopy. *Bio Protoc.* 2017;7(10):e2286. doi: 10.21769/BioProtoc.2286
49. Testa LC, Jule Y, Lundh L, et al. Automated digital quantification of pulmonary fibrosis in human histopathology specimens. *Front Med*. 2021;8:607720. doi: 10.3389/fmed.2021.607720
50. Nguyen TTL, Duong VA, Vo DK, Jo J, Maeng HJ. Development and validation of a bioanalytical LC-MS/MS method for simultaneous determination of sirolimus in porcine whole blood and lung tissue and pharmacokinetic application with coronary stents. *Molecules*. 2021;26(2):425. doi: 10.3390/molecules26020425
51. Baker S, Satish S. Antimicrobial evaluation of fluorescent *Pseudomonas* sp. inhabiting medicinal plant *Annona squamosa* L. *J Pure Appl Microbiol.* 2013;7(2):1027-1033.
52. Ayoubifar M, Abedi F, Nodeh MM, Arasteh O. Pharmacological approach for prevention of bleomycin-induced lung injury. *J Pharm Care.* 2023;11(1):32-39. doi: 10.18502/jpc.v11i1.12638
53. Ayilya BL, Balde A, Ramya M, Benjakul S, Kim SK, Nazeer RA. Insights on the mechanism of bleomycin to induce lung injury and associated in vivo models: a review. *Int Immunopharmacol.* 2023;121:110493. doi: 10.1016/j.intimp.2023.110493
54. Tukhovskaya EA, Palikova YA, Severyukhina MS, et al. Different degrees of expression of pulmonary fibrosis signs with intratracheal administration of bleomycin at different doses in male SD rats (a study aimed at helping to select the optimal bleomycin dose for modeling pulmonary fibrosis). *Front Pharmacol.* 2025;16:1702991. doi: 10.3389/fphar.2025.1702991
55. Rashid RS. Bleomycin lung: a case report. *BMJ Case Rep.* 2009;2009:bcr1120081175. doi: 10.1136/bcr.11.2008.1175
56. Petersen AG, Korntner SH, Bousamaki J, et al. Reproducible lung protective effects of a TGFβR1/ALK5 inhibitor in a bleomycin-induced and spirometry-confirmed model of IPF in male mice. *Physiol Rep.* 2024;12(19):e70077. doi: 10.14814/phy2.70077
57. Tashiro J, Rubio GA, Limper AH, et al. Exploring animal models that resemble idiopathic pulmonary fibrosis. *Front Med*. 2017;4:118. doi: 10.3389/fmed.2017.00118
58. Bordag N, Biasin V, Schnoegl D, et al. Machine learning analysis of the bleomycin mouse model reveals the compartmental and temporal inflammatory pulmonary fingerprint. *iScience*. 2020;23(12):101819. doi: 10.1016/j.isci.2020.101819
59. Pan L, Cheng Y, Yang W, et al. Nintedanib ameliorates bleomycin-induced pulmonary fibrosis, inflammation, apoptosis, and oxidative stress by modulating PI3K/Akt/mTOR pathway in mice. *Inflammation*. 2023;46(4):1531-1542. doi: 10.1007/s10753-023-01825-2
60. Giri SN, Hyde DM, Hollinger MA. Effect of antibody to transforming growth factor beta on bleomycin-induced accumulation of lung collagen in mice. *Thorax*. 1993;48(10):959-966. doi: 10.1136/thx.48.10.959
61. Ishida Y, Kuninaka Y, Mukaida N, Kondo T. Immune mechanisms of pulmonary fibrosis with bleomycin. *Int J Mol Sci.* 2023;24(4):3149. doi: 10.3390/ijms24043149
62. Li Q, Wang Y, Ji L, et al. Cellular and molecular mechanisms of fibrosis and resolution in bleomycin-induced pulmonary fibrosis mouse model revealed by spatial transcriptome analysis. *Heliyon*. 2023;9(12):e22820. doi: 10.1016/j.heliyon.2023.e22461
63. Miao Y, Wang Y, Bi Z, et al. Antifibrotic mechanism of avitinib in bleomycin-induced pulmonary fibrosis in mice. *BMC Pulm Med.* 2023;23(1):94. doi: 10.1186/s12890-023-02385-9
64. Suzuki M, Ikari J, Anazawa R, et al. PAD4 deficiency improves bleomycin-induced neutrophil extracellular traps and fibrosis in mouse lung. *Am J Respir Cell Mol Biol.* 2020;63(6):806-818. doi: 10.1165/rcmb.2019-0433oc
65. Savani RC, Hou G, Liu P, et al. A role for hyaluronan in macrophage accumulation and collagen deposition

after bleomycin-induced lung injury. *Am J Respir Cell Mol Biol.* 2000;23(4):475-484. doi: 10.1165/ajrcmb.23.4.3944

66. Jia K, Wu J, Li Y, et al. A novel pulmonary fibrosis murine model with immune-related liver injury. *Anim Models Exp Med.* 2023;6(3):274-282. doi: 10.1002/ame2.12263
67. Frangogiannis NG. Transforming growth factor-β in tissue fibrosis. *J Exp Med*. 2020;217(3):e20190103. doi: 10.1084/jem.20190103
68. Zheng C, Ding W, Sun Y, Wang Y, Zhang Y. Inhalable albumin nanoparticles co-delivering dihydroartemisinin and nintedanib attenuate pulmonary fibrosis by suppressing TGF-β1/Smad2/3 signaling. *Int J Nanomed.* 2026;21:576680. doi: 10.2147/IJN.S576680
69. Jiang Y, Huang Z, Zhou T, et al. Mitochondria-target ubiquinone attenuates bleomycin-induced pulmonary fibrosis. *Front Pharmacol.* 2025;16:1661644. doi: 10.3389/fphar.2025.1661644
70. Liu T, De Los Santos FG, Phan SH. The bleomycin model of pulmonary fibrosis. In: Rittié L, ed. *Fibrosis: Methods and Protocols.* Methods in Molecular Biology. Vol 1627. Humana Press; 2017:27-42. doi: 10.1007/978-1-4939-7113-8_2
71. Alatawi FS, Omran AM, Rashad E, Abdel-Rahman ON, Soliman AF. Rutin attenuates bleomycin-induced acute lung injury via miR-9-5p-mediated NF-κB signaling inhibition: network pharmacology analysis and experimental evidence. *Front Pharmacol*. 2025;16:1522690. doi: 10.3389/fphar.2025.1522690
72. Adjei-Hinneh G, Adu WA, Ativui S, et al. Diosgenin demonstrates a promising activity by reducing biomarkers related to silica and Mycobacterium-Induced lung inflammation in sprague dawley rats. *SSRN Electronic Journal*. 2024. doi: 10.2139/ssrn.5036676
73. Sherekar P, Suke SG, Dhok A, Harode R, Mangrulkar S, Pingle S. Nano-enabled delivery of diosgenin and emodin ameliorates respirable silica dust-induced pulmonary fibrosis silicosis in rats. *Ecotoxicol Environ Saf*. 2024;279:116483. doi: 10.1016/j.ecoenv.2024.116483
74. Su Y, Che X, Chen Y, et al. Protective role of natural products in pulmonary fibrosis through immunoregulation. *Chin J Nat Med*. 2026;24(1):23-32. doi: 10.1016/S1875-5364(26)61074-6
75. Yang W, Pan L, Cheng Y, et al. Nintedanib alleviates pulmonary fibrosis in vitro and in vivo by inhibiting the FAK/ERK/S100A4 signalling pathway. *Int Immunopharmacol.* 2022;113:109409. doi: 10.1016/j.intimp.2022.109409
76. Putri OK, Wulansari D, Fadlan A, Santoso M, Wiraswati HL, Kusumawati Y. Diosgenin-functionalized zinc oxide nanoparticles produced using Hibiscus tiliaceus leaf extract: evaluation of anticancer and antibacterial activities. *OpenNano*. 2026;27:100274. doi: 10.1016/j.onano.2025.100274
77. Issac PK, Santhi JJ, Janarthanam VA, Velumani K. Diosgenin-conjugated zinc oxide nanoparticles: a sustainable approach to counter antibiotic-induced oxidative stress in the aquatic environment using the in vivo zebrafish larvae model (*Danio rerio*). *BioNanoScience.* 2024;14(2):903-918. doi: 10.1007/s12668-024-01383-3
78. El-Chaghaby GA, Sevindik E, Sevindik M, Kocer O, Uysal I. Humulus species: A traditional medicinal plant and its modern pharmacological importance. *Prospects in Pharmaceutical Sciences*. 2025;23(4):20-28. doi: 10.56782/pps.388